Charge exchange, excitation, and ionization via hidden avoided crossings

T. P. Grozdanov
Institute of Physics, P.O. Box 57, 11001 Beograd, Yugoslavia

E. A. Solov'ev
Institute of Physics, Leningrad State University, U.S.S.R.

(Received 10 April 1990)

General principles of the asymptotic theory of adiabatically slow atomic collisions are reviewed. Special emphasis is placed on analytic properties of adiabatic potential energy curves for complex values of internuclear separation. The significance of the complex branch points and hidden avoided crossings for the dynamics of one-electron collisional systems is discussed. Adiabatic asymptotes of the cross sections for charge exchange, excitation, and ionization in slow $He^{2+}+H(1s)$ and $H^{+}+He^{+}(1s)$ collisions are calculated and compared with other theoretical and experimental data.

I. INTRODUCTION

In the theory of atomic collisions the adiabatic approximation is used for describing inelastic electronic transitions when the collision velocity is small and the nuclear motion can be treated classically. A variant of the adiabatic approximation employed in the collision theory is a further development of the approach of Born and Fock.[1] The exactly solvable models have been considered first: the two-level Landau-Zener model,[2,3] the Rosen-Zener-Demkov model,[4,5] the Nikitin model[6] for the transitions between the bound electronic states, and the Demkov-Osherov[7-9] model for bound-free transitions. These models made it possible not only to calculate a number of physically important processes, but also to construct a more general asymptotic approach in which they appear as partial specific (comparison) problems. The asymptotic theory, first formulated for the two-level nonadiabatic transitions,[10-13] has subsequently been extended to multilevel transitions[14,15] and transitions to the continuum.[16] In this theory there are no assumptions on the specific form of the electronic Hamiltonian, which are present in the exactly solvable models, and only the smallness of the relative nuclear velocity is used. This results in deeper understanding of the nature of nonadiabatic transitions and allows calculations of the processes for which the model treatments are not applicable.

In the present work we report on calculations performed within the framework of the asymptotic theory of nonadiabatic transitions for a number of excitation, charge-exchange, and ionization processes in $He^{2+}+H$ and $H^{+}+He^{+}$ collisions, i.e., for the simplest asymmetric one-electron collision system. The general theory can be found in the review article,[17] but for the sake of completeness and self-consistency, in Secs. II–IV we present some of the results from Ref. 17 in a form which is necessary for understanding the method and the results of our calculations given in Sec. V.

II. GENERAL FORMULATION OF THE PROBLEM; ADIABATIC BASIS COMPATIBLE WITH THE BOUNDARY CONDITIONS

The standard adiabatic wave functions are calculated for fixed positions of the nuclei, and as a consequence they are not compatible with physical boundary conditions imposed at internuclear separations $R\rightarrow\infty$. This incompatibility is due to the fact that such a basis does not contain the Galilean translational factors related to the motion of the nuclei (the so-called electronic momentum transfer problem). As a consequence, in some off-diagonal matrix elements spurious couplings remain at $R\rightarrow\infty$ [see, for example Fig. 2(d) below] and nondecaying transitions between adiabatic states occur. This problem is particularly important in numerical close-coupling calculations which employ adiabatic bases (as shown below, in the asymptotic adiabatic theory it is implicitly assumed that this problem is solved, with no need for explicitly stating how this has been done). At present there are several ways[18-23] of constructing the modified adiabatic bases compatible with physical boundary conditions. Following one of them[19,23] we consider here the case of straight-line motion of the nuclei in the scattering plane (X,Y), $\mathbf{R}=(vt,\rho,0)$, where $v=$const is the relative nuclear velocity along the X axes and ρ is the impact parameter.

Within the classical approximation for the nuclear motion the dynamics of the electron C is described by the time-dependent Schrödinger equation in the center-of-mass system of the nuclei A and B (atomic units $m_e=|e|=\hbar=1$ are used throughout the work, except where explicitly stated otherwise):

$$[-\tfrac{1}{2}\Delta_{\mathbf{r}}+V_{AC}(\mathbf{r}+\gamma_A R)+V_{BC}(\mathbf{r}+\gamma_B R)]\Psi=i\frac{\partial}{\partial t}\Psi\ , \quad (1)$$

where $\gamma_A=\hat{R}M_B/(M_A+M_B)$, $\gamma_B=-\hat{R}M_A/(M_A+M_B)$, $\hat{R}=\mathbf{R}/R$, and $\mathbf{R}$ is the vector connecting nuclei

A and B. The initial condition associated with Eq. (1) is the wave function Ψ, representing the product of the initial atomic wave function $\phi_\alpha^{(a)}(\mathbf{r}_j)$ located at one of the two centers ($j=A,B$) with the Galilean translational factor which takes into account the motion of the nuclei:

$$\Psi(\mathbf{r},t) \underset{t\to-\infty}{\sim} \phi_\alpha^{(a)}(\mathbf{r}_j)\exp[i(\mathbf{v}_j\mathbf{r}_j-\tfrac{1}{2}v_j^2t-E_\alpha^{(a)}t)] , \tag{2}$$

where $\mathbf{r}_j=\mathbf{r}+\boldsymbol{\gamma}_jR$, and $\mathbf{v}_j$ is the velocity of the jth nucleus.

One of the possible ways to solve the problem of momentum transfer is to introduce the nonstationary scaling of the length by substituting $\mathbf{r}$ with the new independent variable

$$\mathbf{q}=\mathbf{r}/R(t) \tag{3}$$

and subsequently transforming to the rotating coordinate system (q_1,q_2,q_3) with the q_1 axis directed along the internuclear axis. In the new coordinate system both potential centers are at rest. In order to transform the Schrödinger equation (1) to the standard form let us represent the wave function as

$$\Psi(\mathbf{r},t)=R^{-3/2}\exp\left[i\frac{r^2\dot{R}}{2R}\right]f(\mathbf{q},t) , \tag{4}$$

where $\dot{R}=dR/dt$ is the radial relative nuclear velocity, and let us introduce a new time variable ($\omega=\rho v$)

$$\tau(t)=\int_0^t\frac{dt'}{R^2(t')}=\omega^{-1}\arctan(vt/\rho) . \tag{5}$$

The factor $R^{-3/2}$ in (4) ensures the normalization and the exponent is the generalized translational factor which takes into account the change in kinematics due to nonstationary length scaling (3). The quantity $\tau\omega$ is the rotation angle of the internuclear axis and the variation of t from $-\infty$ to $+\infty$ corresponds to the variation of τ from $-\pi/(2\omega)$ to $+\pi/(2\omega)$. Substituting (3)–(5) into (1) we obtain the modified Schrödinger equation:

$$Hf(\mathbf{q},\tau)=i\frac{\partial f(\mathbf{q},\tau)}{\partial\tau} , \tag{6}$$

where

$$H=-\tfrac{1}{2}\Delta_{\mathbf{q}}+R^2V_{AC}(R|\mathbf{q}+\boldsymbol{\gamma}_A|)+R^2V_{BC}(R|\mathbf{q}+\boldsymbol{\gamma}_B|)+\omega l_3+\tfrac{1}{2}\omega^2q^2 \tag{7}$$

is the effective Hamiltonian in the new representation, and

$$l_3=i\left[q_1\frac{\partial}{\partial q_2}-q_2\frac{\partial}{\partial q_1}\right] \tag{8}$$

is the operator of the projection of the electronic angular momentum onto the direction perpendicular to the scattering plane.

As mentioned above, in the new coordinates both centers are fixed and there is no momentum-transfer effect. When transforming back to the original wave function Ψ, the correct translational factor is obtained automatically from the exponential factor in (4). Indeed, in the vicinity of the jth center for $R\to\infty$, it is easy to obtain the expression

$$\exp\left[\frac{r^2\dot{\mathbf{R}}}{2R}\right]=\exp\left[i\frac{|\mathbf{r}_j-\boldsymbol{\gamma}_jR|^2\dot{R}}{2R}\right] \underset{Rr_j^{-1}\to\infty}{\sim}\exp[i(\mathbf{v}_j\mathbf{r}_j-\tfrac{1}{2}v_j^2t)] , \tag{9}$$

which is identical to the translational factor in (2).

Let us represent the solution of Eq. (6) in the form of the expansion

$$f(\mathbf{q},\tau)=\sum_\beta g_\beta(\tau)\phi_\beta(\mathbf{q},\tau)\exp\left[-i\int_0^\tau E_\beta(\tau')d\tau'\right] \tag{10}$$

in terms of the eigenfunctions of the effective instantaneous Hamiltonian:

$$H(\tau)\phi_\beta(\mathbf{q},\tau)=E_\beta(\tau)\phi_\beta(\mathbf{q},\tau) . \tag{11}$$

It is natural to call $\phi_\beta(\mathbf{q},\tau)$ the dynamical basis functions and $E_\beta(\tau)$ the dynamical potential energy curves, since besides depending on the internuclear separation R they also depend on $\omega=\rho v$. After the substitution of (10) in (6) the problem is reduced to the solution of the coupled equations for the expansion coefficients $g_\beta(\tau)$:

$$\frac{dg_\beta(\tau)}{d\tau}=\sum_{\gamma(\neq\beta)}W_{\beta\gamma}(\tau)\exp\left[i\int_0^\tau\Delta E_{\beta\gamma}(\tau')d\tau'\right] , \tag{12a}$$

where

$$\Delta E_{\beta\gamma}(\tau)=E_\beta(\tau)-E_\gamma(\tau) , \tag{12b}$$

$$W_{\beta\gamma}(\tau)=\left\langle\phi_\beta\left|\frac{d}{d\tau}\right|\phi_\gamma\right\rangle . \tag{12c}$$

In the present approach the boundary conditions can be formulated in the following way. In the limit $R\to\infty$ the last two terms in the Hamiltonian (7) make no contribution [this can be seen by transforming back (11) to the initial scale of length] and the basis functions ϕ_β tend to atomic functions $\phi_\beta^{(a)}$. Consequently, and also because there is no momentum transfer in the present representation, the population probability amplitudes of atomic states $\phi_\beta^{(a)}$ before and after the collision are identical to $g_\beta(t=\pm\infty)$, and the transition probability from the initial atomic state $\phi_\alpha^{(a)}$ to the final state $\phi_\beta^{(a)}$ is given by

$$P_{\beta\alpha}(\rho,v)=\lim_{t\to+\infty}|g_\beta(\tau)|^2 \tag{13}$$

under the condition

$$\lim_{t\to-\infty}g_\beta(\tau)=\delta_{\alpha\beta} . \tag{14}$$

By intergrating over the impact parameters we obtain the cross section for the inelastic $\alpha\to\beta$ transition:

$$\sigma_{\alpha\beta}(v)=2\pi\int_0^\infty P_{\alpha\beta}(\rho,v)\rho\,d\rho , \tag{15}$$

which is our final goal.

The basis ϕ_β introduced above, apart from the compatibility with the physical boundary conditions, possesses a number of other useful properties. Due to the presence

of the oscillatorlike potential q^2, the spectrum of the effective Hamiltonian (7) is purely discrete, i.e., the functions ϕ_β form a complete discrete basis. The advantage of a discrete basis, as compared to a mixed one containing continuum eigenfunctions, is evident in numerical calculations and is confirmed by the wide use of Sturmian-type bases in many problems of atomic physics. It is easy to show that by using the dynamical basis ϕ_β, the transition probabilities calculated in the center-of-mass frame, laboratory frame, or in a frame centered on either of the nuclei are all equal. All these reference frames differ from each other in new variables (q_1,q_2,q_3) by a constant displacement vector along the q_1 axis. With such a displacement the Hamiltonian H and eigenfunctions ϕ_β are transformed similarly to the gauge transformation in a magnetic field, and the coupled equations (12a) remain invariant. The disadvantage of the basis ϕ_β, as compared to the traditional basis of the two-Coulomb-center problem, is the absence of the separation of variables in Eq. (11) due to the presence of the $l_3\omega$ term in the effective Hamiltonian H (oscillatorlike interaction does not prevent the separation of variables in prolate spheroidal coordinates).

III. ANALYTIC PROPERTIES OF POTENTIAL CURVES AND NONADIABATIC TRANSITIONS

Some general characteristics of the asymptotic theory of nonadiabatic transitions are that not only are the potential curves at real values of internuclear separation used, but some local properties of the corresponding analytically continued functions in the complex R plane are also used. Of course, in a collision process the transitions occur for real R, and the properties of the potential curves for complex values of R enter as a result of approximate (asymptotic) solution of the dynamical problem (1). Here one can make a formal analogy with the approximate calculation of an integral by the saddle-point method, where deforming the contour of integration from the real axis into the complex plane one obtains the value of the integral along the real axis in terms of the values of the integrated function at complex saddle points. Therefore, in the adiabatic approximation, the analyticity of the Hamiltonian as a function of R is of essential importance, since this is the property on which the application of the asymptotic methods relies. In the collision theory this property follows from the R analyticity of the Coulomb interaction of the electrons with nuclei. On the other hand, from the analyticity of the Hamiltonian $H(R)$, it follows that all eigenvalues $E_\beta(R)$ of the given symmetry are different branches of a single analytic function $E(R)$ defined in the entire complex R plane.

At low collision velocities the transitions occur in the regions of avoided crossings (the exact crossing, for real R, of the two potential curves of same symmetry is, according to the Neumann-Wigner theorem,[24] exceptional). An avoided crossing of two potential curves $E_1(R)$ and $E_2(R)$ reflects their exact crossing at complex-conjugate branch points R_c and R_c^* [the eigenvalues obey the obvious relation $E_\beta^*(R^*)=E_\beta(R)$, and consequently all their singular points are distributed in pairs, symmetrically with respect to the real axis]. The degeneracy of the eigenvalues at points R_c and R_c^* is characterized by an important property. Off the real R axis the Hamiltonian is no longer Hermitian and in the case of the equality of two eigenvalues $[E_1(R_c)=E_2(R_c)=E_c]$, in the degenerate subspace for $R=R_c$, it can be reduced to the Jordan form rather than to a diagonal one:[25]

$$H(R_c)=\begin{bmatrix} E_c & 1 \\ 0 & E_c \end{bmatrix} . \tag{16}$$

The eigenvalues $E_1(R)$ and $E_2(R)$ in the vicinity of R_c can be obtained by using the perturbation theory with small parameter $\Delta R=R-R_c$. In the generic case of perturbation linear in ΔR:

$$U(R)=\Delta R\begin{bmatrix} U_{11} & U_{12} \\ U_{21} & U_{22} \end{bmatrix}, \quad U_{ij}=\text{const} \tag{17}$$

the eigenvalues, up to the first order are

$$E_{1,2}=E_c\pm(U_{21}\Delta R)^{1/2} , \tag{18}$$

i.e., instead of the linear small-parameter dependence, as is usual in the perturbation theory, we obtain here the square-root dependence as a consequence of the non-Hermiticity of the Hamiltonian. The square-root branch point connects both potential curves into a single analytic function in such a way that going once around the point R_c the sign is changed in Eq. (18) and the eigenvalues go over into each other. The similar property holds for the corresponding eigenfunctions $\phi_{1,2}$.

Another peculiarity of the Jordan form is that it has only one eigenvector,[25] i.e., when approaching the point R_c not only $E_1\rightarrow E_2$ but also $\phi_1\rightarrow\phi_2$. At first sight, this statement seems to be in contradiction with the orthonormalization condition of the wave functions (below in ϕ_β^*, for real R, we formally substitute R with R^* in order to preserve the analyticity with respect to R of the matrix elements):

$$\int \phi_1(\mathbf{q},R)\phi_1^*(\mathbf{q},R^*)d\mathbf{q}=\int \phi_2(\mathbf{q},R)\phi_2^*(\mathbf{q},R^*)d\mathbf{q}=1 , \tag{19}$$

$$\int \phi_1(\mathbf{q},R)\phi_2^*(\mathbf{q},R^*)d\mathbf{q}=0 . \tag{20}$$

The above conditions can analytically be continued into the complex R plane and, in particular, to the point R_c. Since the wave functions are identical at this point, one might conclude that the same is true for the integrals (19) and (20). However, it can be shown that the wave functions $\phi_{1,2}$ can be represented in the following form:

$$\phi_\beta(\mathbf{q},R)=C_\beta(R)\chi_\beta(\mathbf{q},R) , \tag{21}$$

where $C_\beta(R)$ is a normalization factor which tends to infinity at R_c (see Fig. 1), and $\chi_\beta(\mathbf{q},R)$ is a bounded function for all R with the properties

$$\chi_1(\mathbf{q},R_c)=\chi_2(\mathbf{q},R_c), \quad \int \chi_\beta(\mathbf{q},R_c)\chi_\beta^*(\mathbf{q},R_c^*)d\mathbf{q}=0 . \tag{22}$$

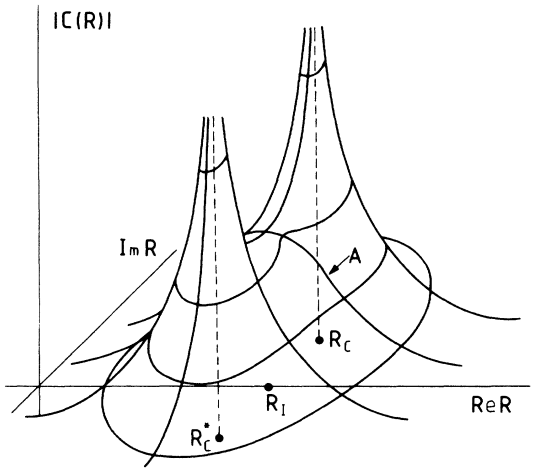

FIG. 1. Singularities of the normalization coefficient $C(R)$ in the complex R plane.

In the orthonormalization conditions the singularity of $C_\beta(R)$ is combined with the zero of matrix element (22) giving indefinite values that are resolved in different ways in the normalization and orthogonality conditions, giving unity in (19) and zero in (20).

The singularity of $C_\beta(R)$ at points R_c and R_c^* induces singularities in all (except normalization) matrix elements, and this leads to a sharp increase of matrix elements for real R in the vicinity of an avoided crossing. Such a behavior is qualitatively illustrated by curve A in Fig. 1. In particular, this explains the bell-shaped profile of the nonadiabatic coupling matrix element [see, for example Fig. 2(d), below].

Summarizing, we emphasize the following logic chain.

(i) Common branch point of a pair of potential curves → (ii) Singularity in normalization factors → (iii) Peak in nonadiabatic coupling matrix element → (iv) Intensive transitions in the region of avoided crossing.

This chain connects the branch points with the nonadiabatic transitions and to some extent qualitatively explains the fact that in the asymptotic theory the transition probability is expressed only through the difference of the potential curves along a line connecting the real R axis with the branch point R_c. On the other hand, this means that all necessary information about the nonadiabatic coupling matrix elements is implicitly contained in the complex potential curves of the problem.

The technique of the asymptotic evaluation of the transition probabilities can in short be described as follows. For $v \to 0$, the solutions of the coupled equations (12a) have in the complex τ plane the following asymptotic behavior:

$$g_\beta(\tau) \sim \exp\left[i \int^{\tau} \Delta E_{\beta\alpha}(\tau') d\tau' \right] , \tag{23}$$

which holds everywhere except in the small region Ω around the complex branch point $\tau_c = \tau(R_c)$. In the region Ω it is necessary to extract and exactly solve the simplified (comparison) system of equations which correctly takes into account the singularities at τ_c of the energy differences and nonadiabatic coupling matrix elements. The asymptotic expression for $g_\beta(\tau)$, uniform in τ, together with the transition-probability amplitude is obtained by matching at the boundary of the region Ω the solution of comparison problem with the asymptotic expression (23) obeying the initial condition (14) (this procedure is completely analogous to calculation of the semiclassical overbarrier reflection coefficient). In the general case of simultaneous avoided crossing of N potential curves, related to an exact crossing at complex point τ_c, the final expression for the transition probability is[14]

$$p_{\beta\alpha} = \left[\frac{\sin[\pi\nu/(N+\nu)]}{\sin[\pi/(N+\nu)]} \right]^2 \exp(-2\Delta_{\beta\alpha}/v) , \tag{24}$$

where

$$\Delta_{\beta\alpha} = \left| \operatorname{Im} \int_{\mathrm{Re}(v\tau_c)}^{v\tau_c} \Delta E_{\beta\alpha}(v\tau) d(v\tau) \right| \tag{25}$$

is the generalized Massey parameter which tends to a constant when $v \to 0$, and ν is the multiplicity of the root τ_c of the difference:

$$\Delta E_{\beta\alpha} \cong \text{const} \times (\tau - \tau_c)^\nu, \quad \beta,\alpha = 1,2,\ldots,N . \tag{26}$$

For the standard two-level avoided crossing, $\nu = \frac{1}{2}$ [see Eq. (18)] and from (24) one obtains the well-known Landau-Zener result with the preexponential factor equal to 1. [For full collision the region of strong nonadiabatic coupling has to be taken into account twice, and an estimate of the full transition probability (averaged over the interference oscillations) is given by $P_{\beta,\alpha} \simeq 2p_{\beta,\alpha}(1 - p_{\beta,\alpha})$.] However, for example, in the case of the two-level rotational Σ-Π transitions, $\nu = 1$,[12,13] and the result is twice the one which would be obtained by the application of the Landau-Zener model with the same Massey parameter.

In the above discussions the eigenvalues involved are the dynamical potential curves of the effective Hamiltonian (7). However, if we confine ourselves to calculation of the transition probabilities accurate up to the leading order in v, which is in complete accord with the asymptotic character of the obtained results, then in the expression for the transition probability (24) we can substitute instead of the dynamical potential curves the usual quasimolecular potential curves. Indeed, when $v \to 0$ ($\omega \to 0$) the last two terms in (7) are small perturbations and the unperturbed part of the Hamiltonian is the quasimolecular Hamiltonian which generates the standard adiabatic basis. In the first-order perturbation theory, the correction to a quasimolecular eigenvalue coming from the oscillatorlike interaction [the last term in (7)] is quadratic in v. The perturbation ωl_3 gives a contribution to E_β only in the second order, because the diagonal matrix elements of this operator in the adiabatic basis are zero due to the symmetry of the unperturbed Hamiltonian with respect

to rotations around the internuclear axis. Therefore the correction associated with ωl_3 is also quadratic in v. As a result, the power expansion in v of the Massey parameter (25) has the following form:

$$\Delta_{\beta\alpha}=\Delta_{\beta\alpha}^{(0)}+v^2\Delta_{\beta\alpha}^{(1)}+O(v^3)\ , \tag{27}$$

where $\Delta_{\beta\alpha}^{(0)}$ is the Massey parameter calculated by using the quasimolecular potential curves.

It should be emphasized that if the power expansion in v of the dynamical eigenvalues contains a linear correction, then it is not possible to calculate transition probability by using only quasimolecular potential curves, because the preexponential factor remains undetermined. Such a situation is realized, for example, for excited states at $R\to 0$ and $R\to\infty$, when the quasimolecular potential curves are degenerate or almost degenerate.

IV. POTENTIAL CURVES IN TWO-COULOMB-CENTER PROBLEM

In the above-discussed asymptotic theory the potential curves are assumed to be known and the question why the avoided crossings occur is not treated at all. We here discuss this question by using as an example the two-Coulomb-center problem, which plays a fundamental role in the atomic collision theory. Usually, the behavior of the potential curves and nonadiabatic coupling matrix elements for real values of R are investigated. That information is necessary for numerical intergration of the molecular-basis close-coupling equations. However, in the asymptotic approach the probabilities for inelastic transitions are expressed in terms of the characteristics of the adiabatic eigenenergies in the complex R plane and general analytic structure of these eigenvalues is of particular importance. Namely, this aspect of the two-Coulomb-center problem (Z_1eZ_2) is discussed below. Earlier investigations of this problem for real values of R led to the conclusion (see, for example, Ref. 26) that in the symmetric case $Z_1=Z_2$ there are no avoided crossings at all. In other words, this would mean that in a collision of such partners like proton and hydrogen the inelastic transitions cannot be explained within the framework of the adiabatic approximation. Only as a result of the direct numerical calculations of the potential curves in the complex R plane for the symmetric case, was it possible to discover new series of branch points and introduce a new type of avoided crossings—the "hidden" avoided crossings.[27] Although they cannot be explicitly seen on graphs of the potential curves for real values of R, only with the help of these avoided crossings is it possible to explain not only the bound-bound transitions but also the ionization process for which the underlying physical mechanism was not known before.

The stationary Schrödinger equation for the two-Coulomb-center problem

$$\left[-\tfrac{1}{2}\Delta-\frac{Z_1}{|\mathbf{r}-\mathbf{R}_1|}-\frac{Z_2}{|\mathbf{r}-\mathbf{R}_2|}\right]\phi_\alpha(\mathbf{r},R)=E_\alpha(R)\phi_\alpha(\mathbf{r},R) \tag{28}$$

allows, as is well known, for the separation of variables in prolate spheroidal coordinates ($r_i=|\mathbf{r}-\mathbf{R}_i|$):

$$\xi=\frac{r_1+r_2}{R},\quad \eta=\frac{r_1-r_2}{R},\quad \varphi=\arctan(x/y)\ ,$$
$$1\le\xi\le\infty,\quad -1\le\eta\le 1,\quad 0\le\varphi\le 2\pi\ . \tag{29}$$

Substitution in (28) of the wave function in the form

$$\phi_\alpha(\mathbf{r},R)=[(\xi^2-1)(1-\eta^2)]^{1/2}F(\xi)G(\eta)\exp(im\varphi) \tag{30}$$

leads to the following equations for the functions $F(\xi)$ and $G(\eta)$:[26]

$$\frac{d^2F(\xi)}{d\xi^2}+\left[-p^2+\frac{a\xi-\lambda}{\xi^2-1}+\frac{1-m^2}{(\xi^2-1)^2}\right]F(\xi)=0\ , \tag{31}$$

$$\frac{d^2G(\eta)}{d\eta^2}+\left[-p^2+\frac{b\eta-\lambda}{1-\eta^2}+\frac{1-m^2}{(1-\eta^2)^2}\right]G(\eta)=0\ , \tag{32}$$

where $p=(-2E)^{1/2}R/2$, $a=(Z_1+Z_2)R$, $b=(Z_1-Z_2)R$, and λ is the separation constant. In classification of states, the united-atom spherical quantum numbers $\alpha=(N,l,m)$ are commonly used (in the limit $R\to 0$, the potential curves of the two-Coulomb-center problem tend to energy levels of the united atom). They are related to the numbers of zeros k,q,m of the wave function in variables ξ,η,φ by the following expressions: $N=k+q+m+1$, $l=q+m$. For l and m we shall also use the spectroscopic notation $l=s,p,d,\ldots$ instead of $l=0,1,2,\ldots$ and $m=\sigma,\pi,\delta,\ldots$ instead of $m=0,1,2,\ldots$.

In the two-Coulomb-center problem there are two nontrivial parameters—internuclear separation $R=|\mathbf{R}_2-\mathbf{R}_1|$ and the ratio of the charges Z_1/Z_2. Let us consider first the symmetric problem $Z_1=Z_2$. In that case the eigenstates are of definite parity with respect to inversions in a coordinate system with the origin at the middle point of the internuclear axis and can be divided into even (g states) and odd (u states). Obviously, the potential curves with different values of m or with different parity cannot have common branch points, since the exact symmetry of the states cannot be changed discontinuously as a result of continuous variation of the parameter R. Figure 2(a) shows the branch points of the potential curves $1s\sigma$ and $2p\sigma$ in molecular ion H_2^+, obtained as a result of numerical calculations.[27,28] As seen from the figure, all branch points can be grouped into two series: S series and T series.

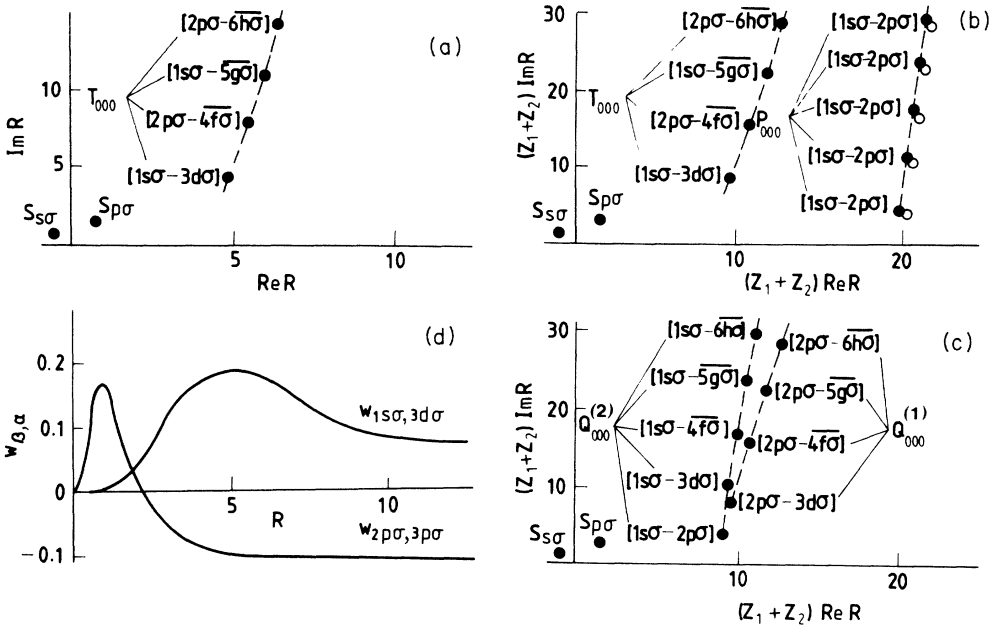

FIG. 2. Branch points of the potential curves $1s\sigma$ and $2p\sigma$ in the complex R plane for three values of the charge Z_2 ($Z_1=1$). The quantum numbers in brackets indicate the pairs of the potential curves connected by the branch points. (a) $Z_2=1$; (b) $Z_2=1.001$, open circles are approximate values obtained by using Eqs. (37) and (38); (c) $Z_2=1.08$. (d) Two examples of matrix elements of the nonadiabatic coupling for the H_2^+ ion (Ref. 37).

A. *S* series of hidden avoided crossings; superpromotion of diabatic potential curves; boundary of the united atom approximation

Any of the S_{lm} series consists of an infinite set of branch points R_N connecting pairwise the potential curves $E_{Nlm}(R)$ and $E_{N+1\,l\,m}(R)$, consecutively for all $N \geq l+1$, and has the following structure. All branch points are localized within the small region Ω in the R plane [on the scale of Fig. 2(a) individual branch points cannot be resolved] and have a limit point

$$R_\infty = \lim_{N\to\infty} R_N \,. \tag{33}$$

In the vicinity of the region Ω (but not within it) the energy surface has the shape of a corkscrew with a pitch decreasing as N^{-3}. Part of this surface, in the case of $S_{p\sigma}$ series, is shown in Fig. 3(a). By associating to each branch point in the given S series an avoided crossing and replacing these avoided crossings with exact crossings we obtain the set of diabatic potential curves which qualitatively illustrate the possible directions of nonadiabatic transitions [see Fig. 3(b)]. As seen from Fig. 3(b), all diabatic potential curves, except one (W_{lm}), behave monotonically. At large R the diabatic level W_{lm} coincides with the lowest adiabatic level in the given series, and with the decrease of R sharply goes upwards crossing the continuum border at $R_S = \mathrm{Re}R_\infty$. Such a behavior has been named "superpromotion," namely, the possibility of the evolution of the system along the diabatic potential curve W_{lm} explains the ionization process in adiabatic approximation.

The appearance of S series of hidden avoided crossings is related to the qualitative changes of the electronic wave function in the vicinity of R_S where the transition from the two-center geometry of the quasimolecule to the single-center geometry of the united atom occurs [see Figs. 4(a) and 4(b)]. Based on such considerations, an approximate analysis of the two-Coulomb-center problem gives a simple and sufficiently accurate analytic expression for the limit point:[29]

$$R_\infty = (Z_1+Z_2)^{-1}\{(l+\tfrac{1}{2})^2 - \tfrac{1}{2}(m+1)^2 \pm i(m+1)[2(l+\tfrac{1}{2})^2 - \tfrac{1}{4}(m+1)^2]^{1/2}\}. \tag{34}$$

The above expression holds equally well for all branch points in the given series (as mentioned above R_N weakly depends on N) and therefore sets the position of a S_{lm} series.

The existence of S series clarifies also the problem of determination of the range of validity of the united-atom approximation. This expansion is widely used in various applications, but it was not clear why in some cases it well approximates the exact potential up to considerable distances, while in other cases the range of validity is extremely small. As is well known, the range of validity is determined by the distance to the nearest singularity. For the united-atom approximation these singularities are in fact the branch points of S series, and the corresponding distance $|R_\infty|$, as seen from (34), strongly depends on l. For example, in the case of the H_2^+ ion, it is

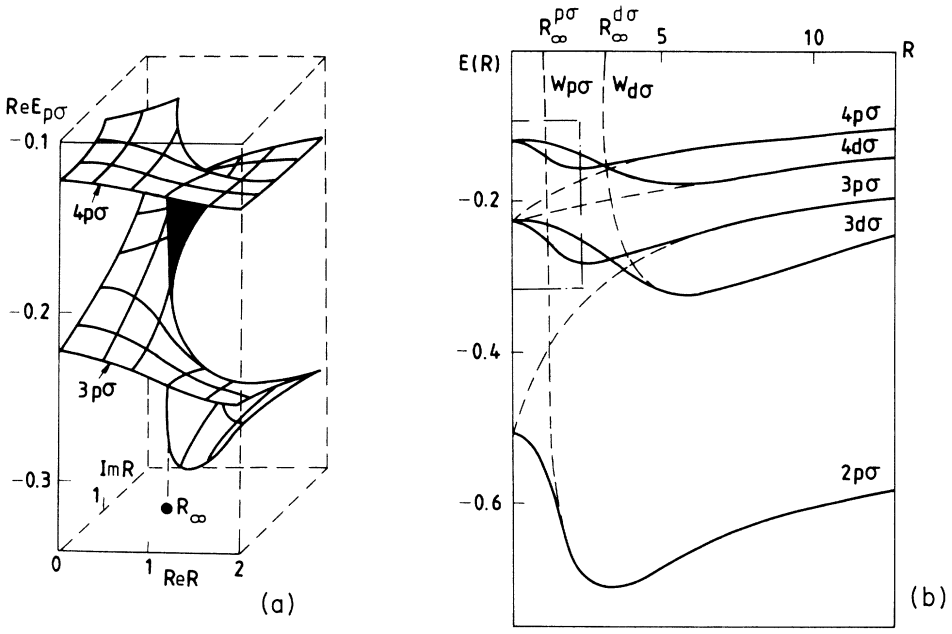

FIG. 3. The region of the S series for the H_2^+ ion. (a) The surface $\mathrm{Re}E_{p\sigma}(R)$ of the multivalued analytic function $E_{p\sigma}(R)$. (b) Adiabatic (solid lines) and diabatic (dashed lines) potential curves. The region indicated by the dot-dashed line corresponds to the front cut of the energy surface in (a).

equal to 17 a.u. for $l=5$, and only 0.5 a.u. for $l=0$.

Another consequence of the existence of S series is the appearance of minima in adiabatic potential energy curves. These minima show up only in potential curves having S series close to the real R axis, i.e., for small m [see Eq. (34)]. Figure 3(a) illustrates formation of minima for the levels $3p\sigma$ and $4p\sigma$ under the influence of $S_{p\sigma}$ series which causes the screwlike form of the energy surface and pulls down the potential curves in the interval $0<R<2R_S$.

B. T series of hidden avoided crossings; boundary of the quasimolecular region

In Fig. 2(a), together with S series there is another series of branch points located around $\mathrm{Re}R\cong 5$ a.u. The merger of two series of branch points associated with $1s\sigma$ and $2p\sigma$ potential curves into a single series is due to the exponential degeneracy of these levels at $R\to\infty$. In the symmetric case ($Z_1=Z_2$), all potential curves are divided into (g,u) pairs, such that at $R\to\infty$, g states go over into

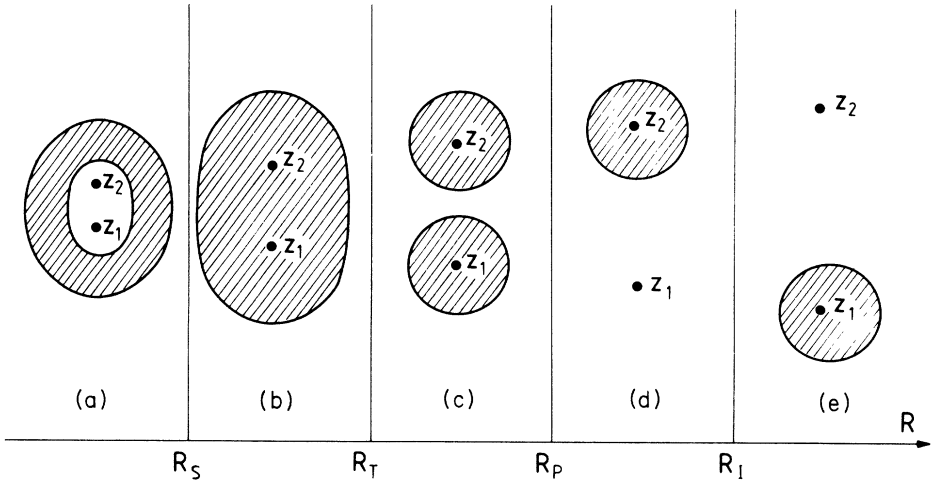

FIG. 4. Qualitative sketch of the classically allowed regions for electronic motion (shaded areas), in the following intervals of the internuclear separations: (a) $0<R<R_S$; (b) $R_S<R<R_T$; (c) $R_T<R<R_P$; (d) $R_P<R<R_I$; (e) $R_I<R<\infty$.

the sum, and u states go over into the difference of the hydrogenic states of isolated atoms (Z_1e) and (Z_2e), having the same set of parabolic quantum numbers (n_1,n_2,m). The relation to the above introduced united-atom quantum numbers is the following:[26]

$$l=m+2n_2-\tfrac{1}{2}[(-1)^m-1],\quad N=q+n_1+m+1 \quad (g \text{ states}), \tag{35}$$

$$l=m+2n_2+\tfrac{1}{2}[(-1)^m+1],\quad N=q+n_1+m+1 \quad (u \text{ states}).$$

As the calculations show each pair has a common series of branch points $T_{n_1n_2m}$ with the higher-lying potential curves. These series have the following properties, illustrated in Fig. 2(a). All branch points of a given series lie on a line, almost perpendicular to the real R axis, with the step $\Delta R \cong 2\pi i n_\infty/(Z_1+Z_2)$ ($n_\infty=n_1+n_2+m+1$ is the principal quantum number of a separated atom Z_ie). The branch points of the g- and u-potential curves alternate and connect the states of the same parity and with the same values of m and quasiradial quantum number k.

The appearance of a T series is related to the promotion of a pair of (g,u)-potential curves to the top of the barrier in the effective potential of quasiangular equation (32). The position of the branch point closest to the real R axis is well approximated by the expressions[30]

$$R_c^{(g)}=6n_\infty(n_\infty-\kappa)+1+4in_\infty \quad (g \text{ terms}),$$
$$R_c^{(u)}=6n_\infty(n_\infty-\kappa)+1+8in_\infty \quad (u \text{ terms}), \tag{36}$$

where $\kappa=k+(m+1)/2$. As in the case of the S series, the existence of the T series is related to the qualitative change of adiabatic states: for $R<R_T=\mathrm{Re}R_c^{(g,u)}$ the electron moves in the common potential well of both centers and its wave function is essentially quasimolecular [see Fig. 4(b)]. For $R>R_T$ the regions of classically allowed motion of the electron in the vicinity of each of the centers are separated by a potential barrier and the wave function can approximately be represented as a (symmetrical or antisymmetrical) superposition of the wave functions corresponding to separated atoms Z_1e and Z_2e [see Fig. 4(c)]. Therefore R_T represents an upper boundary of the quasimolecular region. At the same time, R_T defines the validity range of the asymptotic expansions of potential curves in terms of inverse powers of R.

C. P series of hidden avoided crossings; boundary of approximate (g,u) symmetry

For $Z_1\neq Z_2$ the exact (g,u) symmetry is broken, and additional series of branch points appear. Figure 2(b) shows the branch points of $1s\sigma$ and $2p\sigma$ potential curves for the case $Z_1=1$ and $Z_2=1.001$. Besides the $S_{s\sigma}$, $S_{p\sigma}$, and T_{000} series, a new series labeled P_{000} appears in the region $\mathrm{Re}R\cong 10$ a.u. This series is related to the Rosen-Zener-Demkov type coupling, which is usually considered in the studies of quasiresonant charge-exchange processes. The P series match together the same pairs of potential curves involved in the above-discussed T series. However, these potential curves are not now degenerate in the limit $R\to\infty$, but exhibit the resonance defect:

$$\delta=(Z_2^2-Z_1^2)/(2n_\infty^2) \tag{37}$$

and correspond to parabolic hydrogenic states localized at different centers. The branch points of a $P_{n_1n_2m}$ series can approximately be found within the two-state approximation, by taking for the exchange interaction its asymptotic expression in the two-Coulomb-center problem with unit charges:[31]

$$w(R)=\frac{2(2R/n_\infty)^{n_\infty-n_1+n_2}\exp[-n_\infty-(R/n_\infty)]}{n_\infty^3 n_2!(n_2+m)!}. \tag{38}$$

In this approximation the potential curves are given by

$$E_{1,2}=(Z_1^2+Z_2^2)/(4n_\infty^2)\pm\tfrac{1}{2}[\delta^2+w(R)^2]^{1/2} \tag{39}$$

and the branch points R_c^P can be found as a roots of the transcendental equation $\delta^2+w(R)^2=0$. The results of such a calculation are indicated in Fig. 2(b) as open circles and are in good agreement with the exact values.

The existence of P series is related to the breakdown of the approximate (g,u) symmetry. On the left of such a series ($R<R_p=\mathrm{Re}R_c^P$) it is possible to neglect the resonance defect with respect to the exchange interaction, and the situation is similar to the symmetric case $Z_1=Z_2$, i.e., the adiabatic wave functions are characterized by approximate (g,u) symmetry [see Fig. 4(c)]. On the right of the series ($R>R_P$) the crucial property is the resonance defect, i.e., the asymmetry of the nuclei, so that the approximate symmetry no longer holds and the states are localized at one of the centers [see Fig. 4(d)].

D. Q series of hidden avoided crossings

With further increase of the charge difference $\Delta Z=Z_2-Z_1$, the $S_{s\sigma}$, $S_{p\sigma}$, and T_{000} series at first practically stay at rest, while the P_{000} series moves as a whole to the left and for $\Delta Z=0.07$ the branch points of the P_{000} series pass in between the branch points of the T_{000} series. At that moment the qualitative change of the Riemann surface occurs and the P_{000} series continuously goes over into $Q_{000}^{(2)}$ series, and T_{000} series into $Q_{000}^{(1)}$ [in $Q_{n_1n_2m}^{(i)}$ the superscript $i=1,2$ indicates the atomic complex (Z_ie) to which a given potential curve correlates at $R\to\infty$]. In each of the series of a new type $Q_{000}^{(i)}$, the branch points connect the original potential curve $1s\sigma$ or $2p\sigma$ consecutively with all potential curves having the same value of quasiradial quantum number k [see Fig. 2(c)]. This phenomenon is due to the fact that at $\Delta Z=0.07$ the approximate (g,u) symmetry is destroyed from the outer side down to $R=R_T$, so that the approximately forbidden avoided crossings between the potential curves in T series having the same parity for $Z_1=Z_2$ are

now allowed. Thus, at $\Delta Z=0.07$, the P series, which is characteristic for the Rosen-Zener-Demkov model, disappears and this model is no longer applicable. We note that Rosen-Zener-Demkov coupling disappears at very small values of the resonance defect, constituting only 7% of the energy separation to the closest multiplet.

With further increase of ΔZ, the $1s\sigma$ and $2p\sigma$ potential curves reach the top of the potential barrier at different values of R, and the corresponding $Q^{(2)}_{000}$ series moves to the left and $Q^{(1)}_{000}$ series to the right.

Concerning Figs. 2(a)–2(c), we add the following remark. When a particular branch point $[Nlm\text{-}N'l'm]$ $(N'>N)$ turns out to be on the left or further from the real axis than $S_{l'm}$ series (S_{lm} series is always on the left of such branch point), then starting from the potential curve $E_{Nlm}(R)$ at the real R axis, going around the branch point and returning back to the real R axis, we shall not find ourselves on the potential curve $E_{N'l'm}(R)$, but rather on some antibonding (virtual or quasistationary) potential curve denoted as $\overline{N'l'm}$. Further discussion on antibonding states in the two-Coulomb-center problem can be found in Refs. 17 and 32.

E. Isolated Landau-Zener avoided crossings

In addition to the above-discussed series of branch points, in the two-Coulomb-center problem with $Z_2\neq Z_1$ and $R>R_p$ (or $R>R_Q=\mathrm{Re}R_c^{(i)}$, after the coalescence of T and P series) there are pairs of conjugate branch points R_c and R_c^*, related to the avoided crossings of the usual type between the potential curves of the adiabatic states localized on different centers and characterized asymptotically by the parabolic quantum numbers n_1,n_2,m at center Z_1 and n_1',n_2',m' at center Z_2. Due to the additional dynamical symmetry of the two-Coulomb-center problem,[26] the avoided crossings are allowed only if $k=k'$, $q=q'\pm1$, and $m=m'$. These avoided crossings are known for a long time and have been used for calculations of various processes. The minimal separation between the potential curves $\Delta E_{\min}$ is determined in this case by the underbarrier exchange interaction and therefore the avoided crossings are sharp and clearly visible. For the calculations of the Massey parameter one can use the Landau-Zener approximation:[33]

$$\Delta=\pi\Delta E^2_{\min}/(4\Delta F)\ , \tag{40}$$

where $\Delta F=|F_2-F_1|$ is the slope difference of the corresponding diabatic potential curves at $R_I=\mathrm{Re}R_c$. In Eq. (40), $\Delta E_{\min}$ and ΔF can be substituted by their asymptotic expansions for large values of R. Asymptotic expressions for $\Delta E_{\min}$ have been obtained in semiclassical[34,35] and quantum[36(a),36(b)] approaches. They all give the same accuracy, of the order of 10%. The most compact expression is of the form[35]

$$\Delta E_{\min}=\frac{4E_I(4p_I)^{n_2+n_2'+m+1}\exp(-2p_I)}{[n_\infty n_\infty' n_2!n_2'!(n_2+m)!(n_2'+m)!]^{1/2}}\ , \tag{41}$$

where

$$p_I=\tfrac{1}{2}(-2E_I)^{1/2}R_I,\quad n_\infty'=n_1'+n_2'+m+1\ . \tag{42}$$

The quantities E_I, R_I, and ΔF can be obtained from the expansions of potential curves in inverse powers of R, and in the first approximation are given by

$$E_I=-\frac{(Z_2-Z_1)^2}{2(n_2-n_2')^2}\ ,$$
$$R_I=\frac{2(Z_2-Z_1)}{(Z_2/n_\infty')^2-(Z_1/n_\infty)^2}\ , \tag{43}$$
$$\Delta F=\frac{Z_2-Z_1}{R_I^2}\ .$$

Passing through an isolated avoided crossing is also accompanied by the qualitative change of the adiabatic state. Thus, if for $R<R_I$ the state was localized at center Z_2 [see Fig. 4(d)] then for $R>R_I$ it will be localized at center Z_1 [Fig. 4(e)] and vice versa.

F. Summary

Summarizing the above discussions, we emphasize that the nonadiabatic transitions occur whenever the variation of the internuclear separation is accompanied by the qualitative change of the adiabatic states, i.e., whenever the topology of the classically allowed region for the electronic motion is changed. One might have the impression that S, T, and Q series of branch points play no role in the theory of nonadiabatic transitions, because they do not influence significantly the behavior of the potential curves for real valus of R. However, this is not true. According to the general asymptotic theory any branch point is related to the transition probability (24), which, of course, is the smaller the further the branch point is located from the real R axis. The region of strong nonadiabatic coupling may not be visible on the diagram of the potential curves for real R, as is the case, for example in the Rosen-Zener-Demkov model. More decisive in this respect are the matrix elements of nonadiabatic coupling $w_{\beta,\alpha}(R)$. In Fig. 2(d) two examples[37] of these matrix elements are shown for the case of the H_2^+ ion. As seen from the figure the clearly pronounced maxima appear in the regions where S and T series are located [see Fig. 2(a)], although on the diagram of the potential curves [Fig. 3(b)] no peculiar behavior is visible in these regions.

The approximate expressions (34) and (36) for the positions R_c of the branch points have been obtained within the modified semiclassical approximation.[29,30] They are very useful for obtaining the simple estimates of the cross sections of inelastic processes. The real part of R_c determines the range of impact parameters relevant for the nonadiabatic transitions and the imaginary part is necessary for calculation of the Massey parameter. An estimate of the Massey parameter, for the head-on collisions, can be obtained from the following approximate expressions: in the case of S series,[28]

$$\Delta_{\beta,\alpha}=|\Delta E_{\beta,\alpha}(\mathrm{Re}R_c)\,\mathrm{Im}R_c|\ , \tag{44}$$

and in the cases of T, P, and Q series,

$$\Delta_{\beta,\alpha}=\left|\frac{\pi}{4}\Delta E_{\beta,\alpha}(\mathrm{Re}R_c)\,\mathrm{Im}R_c\right|, \tag{45}$$

where $\Delta E_{\beta,\alpha}$ is the energy difference of the pair of potential curves linked through the branch point R_c. In deriving (45), the following convenient parametrization of the energy difference has been assumed:

$$\Delta E_{\beta,\alpha}(R)=\frac{\Delta E_{\beta,\alpha}(\mathrm{Re}R_c)}{\mathrm{Im}R_c}[(R-R_c)(R-R_c^*)]^{1/2}. \tag{46}$$

The above expression gives the correct energy difference at $R=\mathrm{Re}R_c$ and incorporates the square-root behavior in the vicinity of the complex branch point.

The hidden avoided crossings are broad, characterized by large values of the Massey parameter Δ, and the transitions caused by these avoided crossings become significant at sufficiently high collision velocities v. In connection with this, the question of the validity range of adiabatic approximation arises. In general, there are no quantitative, sufficiently rigorous, validity criteria for the asymptotic expansions. Usually the leading term of the expansion gives satisfactory results even in the region where the first correction becomes larger than the leading term (in that case the first correction should be rejected, since, being only the measure of accuracy, its inclusion will certainly make the result worse). When applied to adiabatic approximation this means that it is justified to extrapolate it to higher values of v, up to $v\cong\Delta$, where the transition probability and the cross section approach the maximum.

V. APPLICATION TO $He^{2+}+H(1s)$ AND $H^+ + He^+(1s)$ COLLISIONS

The ideas presented in the previous sections will now be applied in calculations of the adiabatic asymptotes of the total cross sections for the following processes:

$$He^{2+}+H(1s)\rightarrow He^+(n=2)+H^+ \tag{47}$$

$$\rightarrow He^{2+}+H^+ +e, \tag{48}$$

$$H^+ +He^+(1s)\rightarrow H(1s)+He^{2+} \tag{49}$$

$$\rightarrow H^+ +He^+(n=2) \tag{50}$$

$$\rightarrow H^+ +He^{2+}+e. \tag{51}$$

The charge-exchange processes (47) and (49) are known to be the dominant inelastic channels at low collision velocities. The relevant quasimolecule is $(HeH)^{2+}$ and adiabatic potential energy curves are those of a two-Coulomb-center problem with $Z_1=1$ and $Z_2=2$. The low-lying adiabatic levels are shown in Fig. 5(a), while Fig. 5(b) shows series of branch points in the complex R plane, relevant for the processes (47)–(51). The asymptotic estimates for transition probabilities at $v\rightarrow 0$ are determined by the branch points which lie closest to the real R axis, and these are $R_{1s\sigma,2p\sigma}$, $R_{2p\sigma,3d\sigma}$, and $S_{p\sigma}$ and $S_{d\sigma}$ series. Table I gives the positions of the branch points and the corresponding energy differences, necessary for the calculation of the Massey parameters, as explained below. The positions of the S series have been taken from formula (34) while other parameters have been obtained from numerical calculations.

Any of the branch points $R_{\alpha,\beta}$ belonging to a given Q series connect two surfaces E_α and E_β and the associated single-pass transition probability is [see Eqs. (24) and (25)]

$$p^Q_{\beta,\alpha}=\exp(-2\Delta_{\beta,\alpha}/v), \tag{52}$$

with the Massey parameter given by

$$\Delta_{\beta,\alpha}=\left|\mathrm{Im}\int_{\mathrm{Re}X(R_{\alpha,\beta})}^{X(R_{\alpha,\beta})}\Delta E_{\beta,\alpha}(R(X))dX\right| =\left|\mathrm{Im}\int_C E(R(X))dX\right|, \tag{53}$$

where $E(R)$ is the multivalued analytic function and C is the path in the complex plane of variable $X=vt=(R^2-\rho^2)^{1/2}$, starting at the real X axis [where $E(R)=E_\alpha(R)$], going around the branch point $X_{\alpha,\beta}=X(R_{\alpha,\beta})$ and returning back to the real X axis [where $E(R)=E_\beta(R)$]. For given impact parameter ρ, the integral in (53) can then be calculated numerically by using a program[27] which generates the potential curves of the two-Coulomb-center problem in the complex R plane.

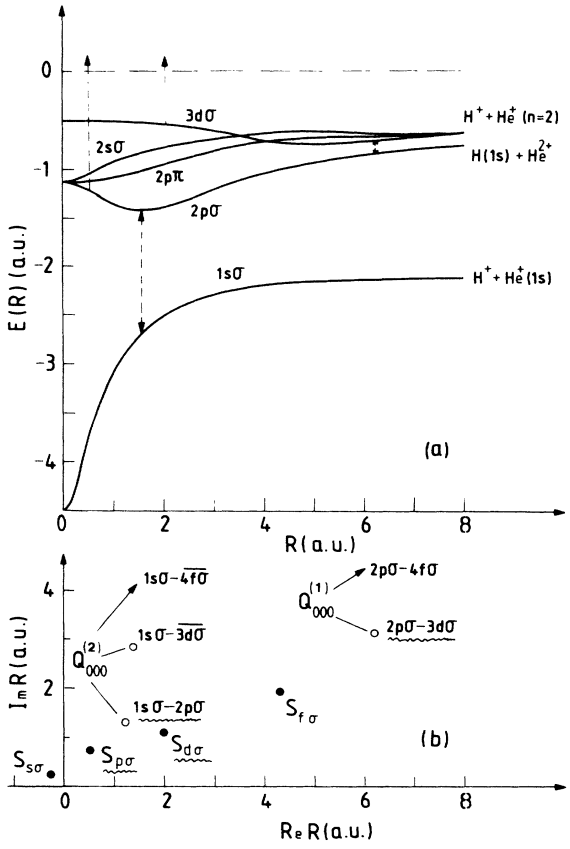

FIG. 5. (a) Low-lying adiabatic potential energy curves of the $(HeH)^{2+}$ quasimolecule. (b) S and Q series of branch points. Underlined are the branch points which govern the processes (47)–(51) and the corresponding transitions are symbolically indicated in (a) by arrows.

TABLE I. Positions in the complex R plane of the branch points $R_{\alpha,\beta}$ of the $Q^{(l)}_{000}$ series and the limiting points R_∞ of the S_{lm} series with the corresponding energies.

(α,β)	$R_{\alpha,\beta}$	lm	R_∞	$E_{l+1\,l\,m}$ (Re R_∞)
$1s\sigma,2p\sigma$	(1.21,1.36)	$p\sigma$	(0.58,0.69)	−1.22
$2p\sigma,3d\sigma$	(6.06,3.14)	$d\sigma$	(1.92,1.17)	−0.56

Each of $S_{lm}=\{R_{l+1},R_{l+2},\ldots,R_\infty\}$ series of branch points is responsible for the population of the whole Rydberg series $\{(l+2,l,m),(l+3,l,m),\ldots\}$, including the transitions to continuum from an initial $(l+1,l,m)$ state. In particular, the probability of the ionization, which, as discussed in Sec. IV A, occurs via the superpromotion of the diabatic W_{lm} potential curve into the continuum in the first half of the collision, can be estimated from the formula[27]

$$P^S_{\infty lm,l+1\,l\,m}=\prod_{N=l+1}^{\infty}\exp\left[-\frac{2\Delta_N}{v}\right]=\exp\left[-\frac{2}{v}\sum_{N=l+1}^{\infty}\Delta_N\right], \tag{54}$$

where

$$\Delta_N=\left|\mathrm{Im}\int_{\mathrm{Re}X(R_N)}^{X(R_N)}[E_{N+1\,l\,m}(R(X))-E_{Nlm}(R(X))]dX\right|. \tag{55}$$

In Eq. (54), it is assumed that the total probability is simply the product of individual probabilities, based on the Demkov-Osherov model.[9] Further simplification relies on the special behavior of $E_{l+1\,l\,m},E_{l+2\,l\,m},\ldots$ energy surfaces in the range of intergration of formula (55). As established in previous numerical calculations,[27] these energy surfaces are nearly constant in this region, except in the close proximity of the branch point R_N. Therefore the limits of integration can, to a good approximation, be replaced, respectively, by $\mathrm{Re}X(R_\infty)$ and $X(R_\infty)$, and E_{Nlm} by their values on the real axes at $R=\mathrm{Re}R_\infty$. Then, in the sum in (54) all terms containing $E_{l+2\,l\,m},E_{l+3\,l\,m},\ldots$ cancel, yielding

$$P^S_{\infty lm,l+1\,l\,m}=\exp\left[-\frac{2}{v}|E_{l+1\,l\,m}(\mathrm{Re}R_\infty)\times\mathrm{Im}(R^2_\infty-\rho^2)^{1/2}|\right]. \tag{56}$$

The S and Q series of branch points shown in Fig. 5(b) are responsible for the transitions between the states of σ symmetry, i.e., they correspond to what is called the radial coupling in the close-coupling approach. In order to have a complete description of the collision dynamics, the transitions involving states of different symmetry should be included, too. They are related to the rotation of the internuclear axis and in the approach of Sec. III would require the knowledge of the dynamical potential curves which include the contribution of the ωl_3 operator in the effective Hamiltonian (7). As also discussed there, these transitions are particularly important in the limit of small and large internuclear separations where the degeneracy of quasimolecular levels of different symmetry occurs.

For the present purposes, we have ignored rotational mixing within the $He^+(n=2)$ manifold at large separations, which predominantly affects only the final sublevel populations in reactions (47) and (50). The $2p\sigma$-$2p\pi$ rotational coupling at small internuclear separations has, however, been included by using the results of Demkov, Kunasz, and Ostrovskii.[38] These authors have proposed a general scaling formula for the σ-π transition probability in the united-atom approximation. In the case of straight-line trajectories it reads

$$P^R_{\pi,\sigma}=\frac{2c_2^2D^2}{2+c_2^2D^2}\exp(-c_1D^3), \tag{57}$$

with

$$c_1=\tfrac{8}{3},\quad c_2=\frac{\pi}{\Gamma(4/3)}(2/3)^{4/3}, \tag{58}$$

$$D=\left[\frac{A}{2v}\right]^{1/3}\rho,\quad A=\frac{(Z_1+Z_2)^2Z_1Z_2}{5N^3}, \tag{59}$$

where N is the united-atom principal quantum number (in our case $Z_1=1$, $Z_2=2$, and $N=2$).

A. $He^{2+}+H(1s)$ collisions

The entrance channel corresponds to the $2p\sigma$ state, and the charge-exchange (CX) process (47) is dominated by the $2p\sigma$-$3d\sigma$ coupling, induced by the branch point $R_{2p\sigma,3d\sigma}$ (see Fig. 5). At close collisions, $2p\sigma$-$2p\pi$ rotational coupling also contributes significantly. The total electron capture probability per collision with given impact parameter can be estimated by summing up individual two-state transition probabilities over the possible reaction paths:

$$P_{\mathrm{CX}}=p^Q_{3d\sigma,2p\sigma}(1-p^Q_{3d\sigma,2p\sigma})+(1-p^Q_{3d\sigma,2p\sigma})P^R_{\pi,\sigma}+(1-p^Q_{3d\sigma,2p\sigma})(1-P^R_{\pi,\sigma})p^Q_{3d\sigma,2p\sigma}. \tag{60}$$

By summing up probabilities in Eq. (60), rather than dealing with quantum amplitudes, we have neglected all interference effects, which is a reasonable approximation as long as we are interested in total (integrated) cross sections. In addition, when writing Eq. (60), all transitions caused by other Q- or S-type branch points (as well as the rotational $3d\sigma$-$3d\pi$-$3d\delta$ coupling) have been neglected in the first approximation.

Figure 6 shows the impact-parameter dependence of the product ρP_{CX} (solid line), calculated from Eq. (60) for He^{2+} impact energy of 0.75 keV/amu. The dashed line shows the result obtained by setting $P^R_{\pi,\sigma}=0$, i.e., by neglecting the rotational $2p\sigma$-$2p\pi$ coupling, which is obviously responsible for the peak at small impact parameters. Also shown in Fig. 6 (dash-dotted line) is the result of Hatton, Lane, and Winter[39] obtained in ten-state molecular-basis with plane-wave translational factors close-coupling calculations. These results are for the capture into all states included in the basis, but at this low

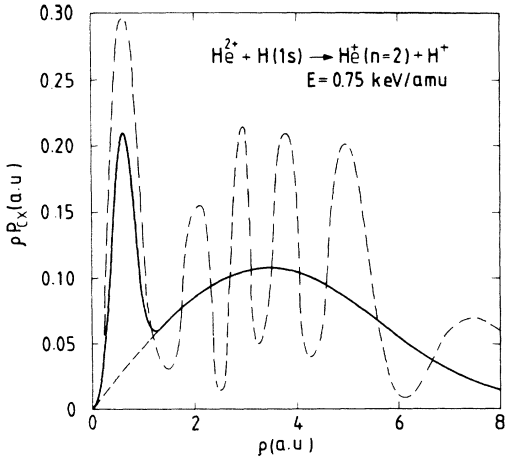

FIG. 6. The product ρP_{CX} vs impact parameter ρ for the charge-exchange process (47). Solid line, present results; dashed line, present results with rotational $2p\sigma$-$2p\pi$ coupling neglected; dot-dashed, results of the molecular close-coupling calculations (Ref. 39).

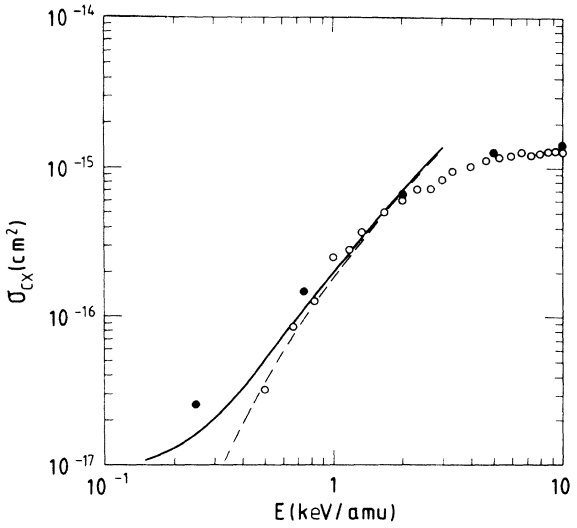

FIG. 7. Cross sections for charge exchange in $He^{2+}+H(1s)$ collisions vs He^{2+} impact energy. Solid line, present results for capture into $He^{+}(n=2)$; dashed line, present results with $2p\sigma$-$2p\pi$ rotational coupling neglected; solid circles, molecular-basis close-coupling calculations for capture into all states of He^{+} (Ref. 39); open circles, experimental data for capture into all states of He^{+} (Ref. 40).

collision velocity they actually correspond to capture into $He^{+}(n=2)$ states. As seen from Fig. 6, the oscillatory ρ dependence, representing the quantum interference effect, is smoothed out in our approach. Although there are differences in the magnitudes of the transition probability at small and large impact parameters, our model seems to incorporate the basic capture mechanism.

Total cross sections for the charge-exchange process (47) at various collision energies are obtained by integrating (60) over the impact parameters. Results are given in Table II and shown in Fig. 7 (solid line). Also shown are the theoretical predictions of Hatton, Lane, and Winter[39] and experimental data of Nutt *et al.*[40] for electron capture into all states of He^{+}. As seen from Fig. 7, our asymptotic result gives a good estimate of the cross section at low energies. The dashed line is obtained by neglecting the $2p\sigma$-$2p\pi$ rotational coupling and indicates that the discrepancy between the theoretical and experimental results at lowest energies is due to the overestimation of the role of the rotational coupling, presumably due to not taking into account the curvature of the classical trajectories.

The ionization process (48) predominantly occurs in the first half of the collision via the sequence of transitions caused by the $S_{d\sigma}$ and $S_{p\sigma}$ series of branch points, after the division of probability flux induced by the $R_{2p\sigma,3d\sigma}$ branch point:

$$P_I = p^{Q}_{3d\sigma,2p\sigma} P^{S}_{\infty d\sigma,3d\sigma} + (1-p^{Q}_{3d\sigma,2p\sigma}) P^{S}_{\infty p\sigma,2p\sigma} \ . \qquad (61)$$

Total ionization cross section as a function of He^{2+} impact energy is given in Table III and shown in Fig. 8. Calculations show that the main contribution comes from the $S_{d\sigma}$ series, while the contribution of the $S_{p\sigma}$ series decreases with increasing energy from 30% to about 10%. Also shown in Fig. 8 are the experimental results of Shah

TABLE II. Cross sections σ_{CX} (in 10^{-16} cm^2) for the charge-exchange process (47) as a functions of the He^{2+} impact energy E (in keV/amu).

E	σ_{CX}
0.2	0.130
0.4	0.329
0.6	0.726
0.8	1.29
1	1.98
1.5	4.14
2.0	6.76
2.5	9.74

TABLE III. Cross sections σ_I (in 10^{-17} cm^2) for the ionization process (48) as a function of the He^{2+} impact energy E (in keV/amu).

E	σ_I
2	2.00[−2][a]
3	8.06[−2]
5	0.343
8	1.02
10	1.61
20	5.39
30	9.77
50	19.0

[a] $a[-b]$ stands for $a \times 10^{-b}$.

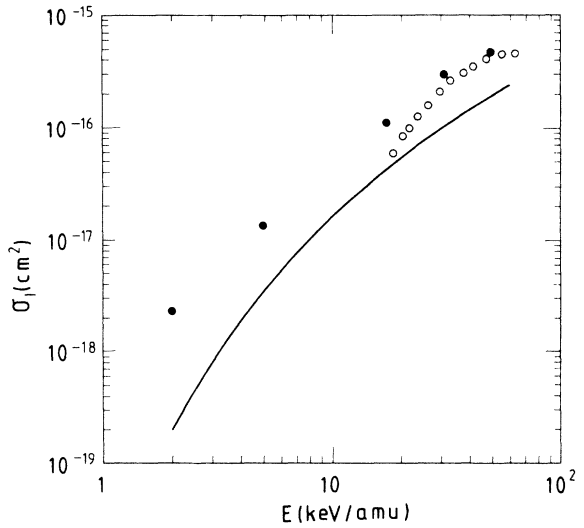

FIG. 8. Cross sections for ionization in $He^{2+}+H(1s)$ collisions vs He^{2+} impact energy. Solid line, present results; solid circles, triple-center pseudostate close-coupling calculations (Ref. 42); open circles, experiment (Ref. 41).

et al.[41] and the theoretical predictions of Winter[42] obtained by the triple-center pseudostate close-coupling calculations. Our results predict lower cross sections. The reason for this could be the omission in our treatment of another possible ionization mechanism. This mechanism[30] is related to excitation (an eventually ionization) of the electron in the second half of the collision (at large internuclear separations) via the sequence of nonadiabatic transitions, such as $2p\sigma \rightarrow 3d\sigma, 3d\sigma \rightarrow 4f\sigma, \ldots, (l, l-1, \sigma) \rightarrow (l+1, l, \sigma), \ldots$, associated with the closest to the real R-axis members of various Q series. This mechanism corresponds to the excitation of an electron localized at the top of the potential barrier in quasiangular equation (32), i.e., near the saddle point of the three-dimensional potential. It should also be noted that the low-energy results of Winter shown in Fig. 8 (for $E=2$ and 5 keV/amu) are not converged and have the tendency of decreasing with increasing the size of the basis.[42] The trend of the experiment also suggests that the triple-center calculations overestimate cross sections at low energies.

B. $H^+ + He^+(1s)$ collisions

In this case the initial quasimolecular state is $1s\sigma$. The charge-exchange process (49) proceeds mainly via the $1s\sigma \leftrightarrow 2p\sigma$ transitions induced by the $R^Q_{1s\sigma,2p\sigma}$ branch point (see Fig. 5), with a part of probability flux taken away by the rotational $2p\sigma$-$2p\pi$ transitions at small separations and by $2p\sigma \rightarrow 3d\sigma$ transitions at large separations in the second half of the collision:

$$P_{CX} = p^Q_{2p\sigma,1s\sigma}(1-P^R_{\pi,\sigma})(1-p^Q_{2p\sigma,1s\sigma})(1-p^Q_{3d\sigma,2p\sigma}) + (1-p^Q_{2p\sigma,1s\sigma})p^Q_{2p\sigma,1s\sigma}(1-p^Q_{3d\sigma,2p\sigma}) \ . \tag{62}$$

The most probable competitive process is the excitation (EX) [Eq. (50)], which involves the contributions from the same branch points:

$$P_{EX} = p^Q_{2p\sigma,1s\sigma}P^R_{\pi,\sigma} + p^Q_{2p\sigma,1s\sigma}(1-P^R_{\pi,\sigma})(1-p^Q_{2p\sigma,1s\sigma})p^Q_{3d\sigma,2p\sigma} + (1-p^Q_{2p\sigma,1s\sigma})p^Q_{2p\sigma,1s\sigma}p^Q_{3d\sigma,2p\sigma} \ . \tag{63}$$

The calculated cross sections as functions of the collision energy in the center-of-mass frame for the processes (49) and (50) are given in Table IV and shown in Figs. 9 and 10 ($E_{c.m.}=0.8E$, where E is the proton energy relative to $^4He^+$ ion).

Also shown in Fig. 9 are the results of molecular-basis close-coupling calculations of Kimura and Thorson[43] (solid squares) and of Winter, Hatton, and Lane[44] (crosses), the Sturmian-basis close-coupling results of Winter[45] (solid circles), as well as the experimental data of Peart, Grey, and Dolder[46] and Rinn, Melchert, and Salzborn[47] (open symbols) for electron capture into all states of H. As seen from the figure, our asymptotic estimate for the dominant charge-exchange channel (49) (solid line) is reasonably good, especially at low energies.

In Fig. 10 our results (solid line) for the excitation process (50) agree well with the molecular close-coupling calculations of Kimura and Thorson[43] (solid squares) and Winter, Hatton, and Lane[44] (crosses). At higher energies our predictions presumably overestimate true cross sections, since, as seen from Table IV, the excitation cross section becomes larger than the electron capture cross section.

The basic mechanism responsible for the ionization process (51) is the electron promotion into the continuum in the first half of the collision, via the sequence of transitions induced by the $S_{p\sigma}$ series of branch points, after the $1s\sigma \rightarrow 2p\sigma$ transition:

$$P_I = p^Q_{2p\sigma,1s\sigma}P^S_{\infty p\sigma,2p\sigma} \ . \tag{64}$$

The calculated cross sections are given in Table V and shown in Fig. 11, together with the experimental data of Watts, Dunn, and Gilbody[48] (open squares) and Rinn *et al.*[49] (open circles), the theoretical results of atomic-orbital-pseudostate[50] (solid triangles), Sturmian[51] (crosses), and triple-center-pseudostate[42] (solid circles) calculations. The agreement with our asymptotic results is reasonably good, although the same remarks hold, as in the above-discussed case of ionization in $He^{2+}+H$ col-

TABLE IV. Cross sections σ_{CX} (in 10^{-18} cm^2) for the charge-exchange process (49), and σ_{EX} (in 10^{-18} cm^2) for the excitation process (50) as functions of the center-of-mass energy $E_{c.m.}$ (in keV).

$E_{c.m.}$	σ_{CX}	σ_{EX}
1.5	2.97[−3][a]	6.67[−4]
3	7.85[−2]	2.83[−2]
5	0.472	0.244
8	1.72	1.22
10	2.89	2.38
15	6.44	6.87
20	10.4	13.2
30	18.2	29.6

[a] $a[-b]$ stands for $a \times 10^{-b}$.

lision. The experimental results are rather uncertain, especially at lower energies, since they have been obtained as a difference of the measured cross sections for the He^{2+} production and the charge exchange (see, e.g., Ref. 49). The ionization process (51) has previously been treated by the present authors,[52] assuming a simplified model [see Eq. (46)] for $\Delta E_{2p\sigma,1s\sigma}(R)$ in the complex R plane. Present cross sections, obtained by numerical evaluation of the Massey parameter (53) with the exact adiabatic potential curves, are about 50% larger.

VI. CONCLUDING REMARKS

At the present time, the theoretical investigations of electronic transitions in atomic collisions are to a large extent reduced to a numerical solution of close-coupling equations and development of packages of programs for automatic calculations of cross sections (see, for example, Refs. 42 and 51). However, in the region of slow collisions, where the transition probabilities are small, this approach becomes more complicated due to the presence of nonphysical transitions related to the incompleteness of the basis functions. These transitions, being accumulated during the intergration of the coupled equation, can significantly change the true value of the transition probability. On the other hand, the asymptotic theory considered in the present work has no problems of this kind. This theory also provides important information: why and at what internuclear separations a particular process predominantly occurs. Wider application of the adiabatic approximation has been limited in the past due to the absence of the general method for determination of the avoided crossings connecting the given initial and final states. In practice, the only transitions considered were

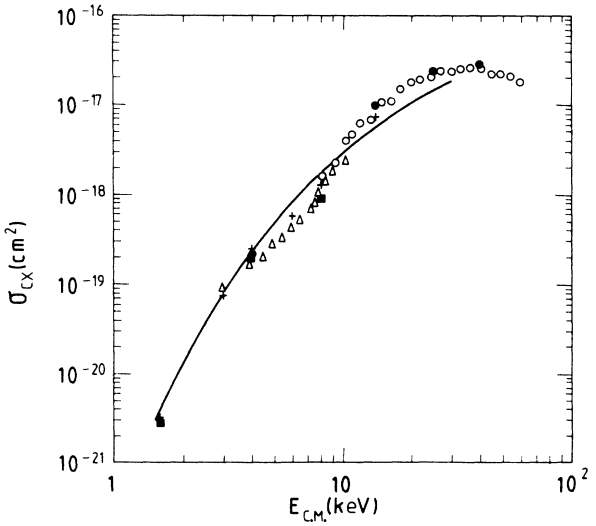

FIG. 9. Cross sections for charge exchange in $H^+ + He^+(1s)$ collisions vs collision energy in the center-of-mass frame. Solid line, present results for capture into H(1s); solid squares and crosses, molecular close-coupling calculations (Refs. 43 and 44, respectively); solid circles, Sturmian close-coupling calculations (Ref. 45); open triangles and circles, experiment (Refs. 46 and 47, respectively).

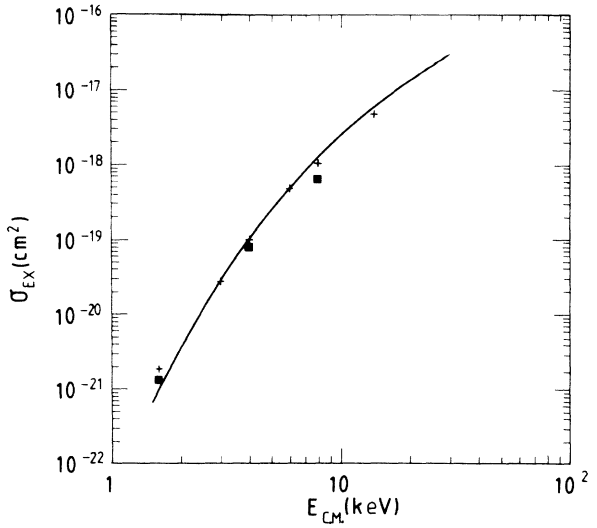

FIG. 10. Cross sections for excitation of $He^+(n=2)$ in $H^+ + He^+(1s)$ collisions vs center-of-mass collision energy. Solid line, present results; solid squares and crosses, molecular close-coupling calculations (Refs. 43 and 44, respectively).

TABLE V. Cross sections σ_I (in 10^{-18} cm^2) for the ionization process (51) as a function of the center-of-mass energy $E_{c.m.}$ (in keV).

$E_{c.m}$	σ_1
4	1.08[−3][a]
6	8.52[−3]
8	2.99[−2]
15	0.286
20	0.672
40	3.70
60	8.36
80	14.0

[a] $a(-b)$ stands for $a \times 10^{-b}$.

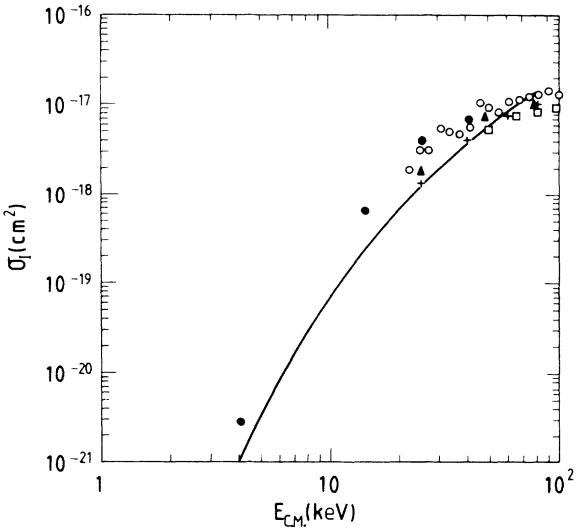

FIG. 11. Cross sections for ionization in $H^+ + He^+(1s)$ collisions vs center-of-mass collision energy. Solid line, present results; solid triangles, atomic-orbital pseudostate calculations (Ref. 50); crosses, Sturmian pseudostate calculations (Ref. 51); solid circles, triple-center pseudostate calculations (Ref. 42); open circles and squares, experiment (Refs. 48 and 49, respectively).

those of Landau-Zener or Rozen-Zener-Demkov type which are induced by the underbarrier resonant interactions of the states localized on different centers. As a result, the conclusions were drawn, such as that in the quasimolecule H_2^+ there are no avoided crossings. However, with the discovery of the S, T, P, and Q series of hidden avoided crossings, it is possible to obtain the complete description of inelastic transitions within the framework of the adiabatic approximation for the simplest quasimolecular system Z_1eZ_2. The analysis of this system points towards the universal method for describing the hidden avoided crossings. As was shown in Ref. 30, in the Z_1eZ_2 problem the hidden avoided crossings occur whenever the adiabatic state, in the classical limit, can be related to an unstable periodic orbit. An approach based on the investigation of periodic orbits and associated monodromy matrices does not require the separation of variables and would be applicable in a general case.

Concerning the general approach of Sec. II, more detailed studies of the dynamical states and eigenvalues related to the effective Hamiltonian (7) are necessary. The first step would consist in considering the limiting cases $R \to 0$ and $R \to \infty$, where analytic treatments seem to be possible.

ACKNOWLEDGMENTS

T.P.G. acknowledges the support to this work by the U.S. National Institute of Standards and Technology and SIZ Nauke Srbije through the U.S.-Yugoslav Joint Board of Scientific and Technological Cooperation (Contract No. NIST JF 691) and by the International Atomic Energy Agency, Vienna (Contract No. 5329/R1/RB).

[1]M. Born and V. Fock, Z. Phys. **51**, 165 (1928).
[2]L. D. Landau, Phys. Z. Sowjetunion. **1**, 88 (1932).
[3]C. Zener, Proc. R. Soc. **40**, 696 (1932).
[4]N. Rosen and C. Zener, Phys. Rev. **40**, 502 (1932).
[5]Yu. N. Demkov, Zh. Eksp. Teor. Fiz. **45**, 195 (1963) [Sov. Phys.—JETP **18**, 138 (1964)].
[6]E. E. Nikitin, Opt. Spektrosk. **13**, 761 (1962) [Opt. Spectrosc. (USSR) **13**, 431 (1962)].
[7]V. I. Osherov, Zh. Eksp. Teor. Fiz. **49**, 1157 (1965) [Sov. Phys.—JETP **22**, 804 (1966)].
[8]Yu. N. Demkov, Dokl. Akad. Nauk SSSR **166**, 1076 (1966) [Sov. Phys.—Dokl. **11**, 138 (1966)].
[9]Yu. N. Demkov and V. I. Osherov, Zh. Eksp. Theor. Fiz. **53**, 1589 (1967) [Sov. Phys.—JETP **26**, 916 (1968)].
[10]E. C. G. Stueckelberg, Helv. Phys. Acta **5**, 369 (1932).
[11]A. M. Dykhne, Zh. Eksp. Teor. Fiz. **41**, 1324 (1961) [Sov. Phys.—JETP **14**, 941 (1962)].
[12]E. A. Solov'ev, Vestn. Leningr. Univ. Fiz. **4**, 10 (1976).
[13]A. T. Voronin, S. P. Karkach, V. I. Osherov, and V. G. Ushakov, Zh. Eksp. Teor. Fiz. **71**, 884 (1976) [Sov. Phys.—JETP **44**, 465 (1976)].
[14]E. A. Solov'ev, Teor. Mat. Fiz. **28**, 115 (1976) [Theor. Math. Phys. (USSR) **28**, 669 (1976)].
[15]E. A. Solov'ev, Teor. Mat. Fiz. **32**, 373 (1977) [Theor. Math. Phys. **32**, 803 (1977)].
[16]E. A. Solov'ev, Zh. Eksp. Teor. Fiz. **70**, 872 (1976) [Sov. Phys.—JETP **43**, 453 (1976)].
[17]E. A. Solov'ev, Usp. Fiz. Nauk **157**, 437 (1989) [Sov. Phys.—Usp. **32**, 228 (1989)].
[18]D. Bates and D. A. Williams, Proc. Phys. Soc. **83**, 425 (1964).
[19]E. A. Solov'ev, Teor. Mat. Fiz. **28**, 240 (1976) [Theor. Math. Phys. (USSR) **28**, 575 (1976)].
[20]S. B. Schneiderman and A. Russek, Phys. Rev. **181**, 311 (1969).
[21]J. B. Delos, Rev. Mod. Fiz. **53**, 287 (1981).
[22]L. F. Errea, L. Mendez, and A. Riera, J. Phys. B **15**, 101 (1982).
[23]E. A. Solov'ev and S. I. Vinitsky, J. Phys. B **18**, L557 (1985).
[24]J. Neuman and E. Wigner, Phys. Z. **30**, 467 (1929).
[25]A. P. Mishin and I. V. Proskuryakov, *Higher Algebra* (Fizmatgiz, Moskva, 1962) (in Russian).
[26]I. V. Komarov, L. I. Ponomarev, and S. Yu. Slavyanov, *Spheroidal and Coulomb Spheroidal Functions* (Nauka, Moskva, 1976) (in Russian).
[27]E. A. Solov'ev, Zh. Exp. Theor. Fiz. **81**, 1681 (1981) [Sov. Phys.—JETP **54**, 893 (1981)].
[28]S. Yu. Ovchinikov and E. A. Solov'ev, Zh. Eksp. Teor. Fiz. **90**, 921 (1986) [Sov. Phys.—JETP **63**, 538 (1986)].
[29]E. A. Solov'ev, Zh. Eksp. Teor. Fiz. **90**, 1165 (1986) [Sov. Phys.—JETP **63**, 678 (1986)].
[30]D. I. Abramov, S. Yu. Ovchinikov, and E. A. Solov'ev (unpublished).
[31]B. M. Smirnov, Zh. Eksp. Teor. Fiz. **46**, 1017 (1964) [Sov. Phys.—JETP **19**, 692 (1964)].
[32]S. Yu. Ovchinikov and E. A. Solov'ev, Zh. Eksp. Teor. Fiz. **91**, 477 (1986) [Sov. Phys.—JETP **64**, 280 (1986)].

[33]L. D. Landau and E. M. Lifshitz, *Quantum Mechanics, Non-Relativistic Theory* (Pergamon, New York, 1977).
[34]L. I. Ponomarev (unpublished).
[35]P. T. Greenland, J. Phys. B **11**, 3563 (1978).
[36](a) I. V. Komarov and E. A. Solovev, Teor. Mat. Fiz. **40**, 130 (1979) [Theor. Math. Phys. (USSR) **40**, 645 (1979)]; (b) T. P. Grozdanov, R. K. Janev, and V. Yu. Lazur, Phys. Rev. A **32**, 25 (1985).
[37]L. I. Ponomarev, T. P. Puzinina, and N. F. Truskova, J. Phys. B **11**, 3861 (1978).
[38]Yu. N. Demkov, C. V. Kunasz, and V. N. Ostrovskii, Phys. Rev. A **18**, 2097 (1978).
[39]G. J. Hatton, N. F. Lane, and T. G. Winter, J. Phys. B **12**, L571 (1979).
[40]W. L. Nutt, R. W. McCullough, K. Brady, M. B. Shah, and H. B. Gilbody, J. Phys. B **11**, 1457 (1978).
[41]M. B. Shah, D. S. Elliot, P. McCallion, and H. B. Gilbody, J. Phys. B **21**, 2455 (1988).
[42]T. G. Winter, Phys. Rev. A **37**, 4656 (1988).
[43]M. Kimura and W. R. Thorson, Phys. Rev. A **24**, 3019 (1981).
[44]T. G. Winter, G. J. Hatton, and N. F. Lane, Phys. Rev. A **22**, 930 (1980).
[45]T. G. Winter, Phys. Rev. A **33**, 3842 (1986).
[46]B. Peart, R. Grey, and K. Dolder, J. Phys. B **16**, 2675 (1977).
[47]K. Rinn, F. Melchert, and E. Salzborn, J. Phys. B **18**, 3783 (1985).
[48]M. F. Watts, K. F. Dunn, and G. B. Gilbody, J. Phys. B **19**, L355 (1986).
[49]K. Rinn, F. Melchert, K. Rink, and E. Salzborn, J. Phys. B **19**, 3717 (1986).
[50]W. Fritch and C. D. Lin, in *Abstracts of Contributed Papers, Thirteenth International Conference of the Physics of Electronic and Atomic Collisions, Berlin, 1983,* edited by J. Eichler, W. Fritsch, I. V. Hertel, N. Stolterfoht, and U. Wille (ICPEAC, Berlin, 1983), p. 502.
[51]T. G. Winter, Phys. Rev. A **35**, 3799 (1987).
[52]T. P. Grozdanov and E. A. Solov'ev, Phys. Rev. A **38**, 4333 (1988).